J Physiol 591.18 (2013) pp 4459–4472

The Journal of Physiology

The mechanism underlying maintenance of the endocochlear potential by the K^+ transport system in fibrocytes of the inner ear

Naoko Adachi[1,3], Takamasa Yoshida[4,5,6], Fumiaki Nin[1,3,5,6], Genki Ogata[5,6], Soichiro Yamaguchi[5], Toshihiro Suzuki[3], Sizuo Komune[4], Yasuo Hisa[3], Hiroshi Hibino[5,6] and Yoshihisa Kurachi[1,2]

[1]*Division of Molecular and Cellular Pharmacology, Department of Pharmacology, Graduate School of Medicine, and* [2]*The Center for Advanced Medical Engineering and Informatics, Osaka University, 2-2 Yamada-oka, Suita, Osaka 565-0871, Japan*
[3]*Department of Otolaryngology-Head and Neck Surgery, Kyoto Prefectural University of Medicine, Kyoto, Japan*
[4]*Department of Otorhinolaryngology, Graduate School of Medical Sciences, Kyushu University, Kyushu, Japan*
[5]*Department of Molecular Physiology, Niigata University School of Medicine, Niigata, Japan*
[6]*Center for Transdisciplinary Research, Niigata University, Niigata, Japan*

Key points

- The endocochlear potential (EP) of +80 mV in cochlear endolymph is essential for audition and controlled by K^+ transport across the lateral cochlear wall composed of two epithelial barrier layers, the syncytium containing the fibrocytes and the marginal cells.
- The EP depends upon the diffusion potential elicited by a large K^+ gradient across the apical surface of the syncytium.
- We examined by electrophysiological approaches an involvement of Na^+,K^+-ATPase, which occurs at the syncytium's basolateral surface comprising the fibrocytes' membranes and would mediate K^+ transport across the lateral wall, in maintenance of the EP.
- We show that the Na^+,K^+-ATPase sustains the syncytium's high $[K^+]$ that is crucial for the K^+ gradient across the apical surface of the syncytium.
- The results help us better understand the mechanism underlying the establishment of the EP as well as the pathophysiological process for deafness induced by dysfunction of the ion transport apparatus.

Abstract The endocochlear potential (EP) of +80 mV in the scala media, which is indispensable for audition, is controlled by K^+ transport across the lateral cochlear wall. This wall includes two epithelial barriers, the syncytium and the marginal cells. The former contains multiple cell types, such as fibrocytes, which are exposed to perilymph on their basolateral surfaces. The apical surfaces of the marginal cells face endolymph. Between the two barriers lies the intrastrial space (IS), an extracellular space with a low K^+ concentration ($[K^+]$) and a potential similar to the EP. This intrastrial potential (ISP) dominates the EP and represents the sum of the diffusion potential elicited by a large K^+ gradient across the apical surface of the syncytium and the syncytium's potential, which is slightly positive relative to perilymph. Although a K^+ transport system in fibrocytes seems to contribute to the EP, the mechanism remains uncertain. We examined the electrochemical properties of the lateral wall of guinea pigs with electrodes sensitive to potential and K^+ while perfusing into the perilymph of the scala tympani blockers of Na^+,K^+-ATPase, the K^+ pump thought to be essential to the system. Inhibiting Na^+,K^+-ATPase barely affected $[K^+]$ in the IS but greatly decreased $[K^+]$ within the syncytium, reducing the K^+ gradient across its

N. Adachi and T. Yoshida contributed equally to this study.

DOI: 10.1113/jphysiol.2013.258046

apical surface. The treatment hyperpolarized the syncytium only moderately. Consequently, both the ISP and the EP declined. Fibrocytes evidently use the Na^+,K^+-ATPase to achieve local K^+ transport, maintaining the syncytium's high [K^+] that is crucial for the K^+ diffusion underlying the positive ISP.

(Received 2 May 2013; accepted after revision 3 July 2013; first published online 8 July 2013)

Corresponding authors H. Hibino: Department of Molecular Physiology, Niigata University School of Medicine, 1-757 Asahimachi-dori, Chuo-ku, Niigata, Niigata 951-8510, Japan. Email: hibinoh@med.niigata-u.ac.jp
Y. Kurachi: Division of Molecular and Cellular Pharmacology, Department of Pharmacology, Graduate School of Medicine, Osaka University, 2-2 Yamada-oka, Suita, Osaka 565-0871, Japan. Email: ykurachi@pharma2.med.osaka-u.ac.jp

Abbreviations *a*K^+, K^+ activity; BC, basal cell; ClC-K, Cl^- channels ClC-K/barttin; EL, endolymph; EP, endocochlear potential; IC, intermediate cell; IS, intrastrial space; ISP, intrastrial potential; MC, marginal cell; NKCC, Na^+,K^+,2Cl^--cotransporters; PL, perilymph; TJ, tight junction.

Introduction

The mammalian cochlea harbours three tubular chambers: the scala vestibuli and scala tympani containing an ordinary extracellular fluid, perilymph; and the scala media filled with a unique solution, endolymph (Fig. 1*A*). Endolymph contains 150 mM K^+ and shows an endocochlear potential (EP) of +80 mV relative to perilymph and other extracellular fluids including plasma (von Békésy, 1952; Hibino & Kurachi, 2006). The sensory hair cells upon the basilar membrane bathe their basolateral surfaces in perilymph and expose their apical surfaces, which are surmounted by stereocilia, to endolymph. Sound-induced vibration of the basilar membrane deflects the stereocilia and opens mechanosensitive channels that permit K^+ influx (Hudspeth, 1989). The positive EP facilitates the K^+ current and sensitizes hair cells by enhancing the driving force. K^+ exits the hair cells into the perilymph of the scala tympani and returns to the endolymph of the scala media through the lateral cochlear wall comprising the spiral ligament and the stria vascularis (Fig. 1*A*; Wangemann, 2006; Zdebik *et al.* 2009).

The lateral cochlear wall is made up of multiple cell types (Fig. 1*B*). Marginal cells, which are connected laterally by tight junctions, constitute a monolayered barrier whose apical surface faces the endolymph. Fibrocytes, the major constituents of the spiral ligament, strial intermediate cells and basal cells are interconnected by gap junctions and constitute an electrochemical 'syncytium' (Wangemann *et al.* 1995; Takeuchi & Ando, 1998; Takeuchi *et al.* 2000; Cohen-Salmon *et al.* 2007). Tight junctions between the basal cells make the syncytium a diffusional barrier and serve as the boundary for the apical surface composed of intermediate cell membranes and the basolateral surface comprising the fibrocyte membranes. These two barriers were proposed in a two-cell model (Wangemann *et al.* 1995) and a subsequent five-compartment model (Takeuchi *et al.* 2000). Between the two systems there exists a 15 nm extracellular separation, the intrastrial space (IS), that is penetrated by numerous capillaries (Fig. 1*B*; Hinojosa & Rodriguez-Echandia, 1966; Takeuchi *et al.* 2000; Spicer & Schulte, 2005; Wangemann, 2006; Hibino *et al.* 2010).

The stria vascularis, which includes the intermediate and basal cells of the syncytium, the IS and the marginal cells, is essential for establishing the EP (Tasaki & Spyropoulos, 1959). Previous electrophysiological studies suggested that a K^+ conductance in the stria vascularis is involved in generation of the EP (Marcus *et al.* 1985). The fluid of the IS has a low K^+ concentration ([K^+]) and a positive potential similar to the EP (Salt *et al.* 1987; Ikeda & Morizono, 1989). This IS potential (ISP) was proposed to be the origin of the EP and to represent primarily a K^+ diffusion potential (Salt *et al.* 1987; Takeuchi *et al.* 2000). We demonstrated recently that the ISP dominates the EP and is sustained by the electrical isolation of the IS from the neighbouring perilymph, blood and endolymph (Nin *et al.* 2008). The ISP is formed by K^+ diffusion through inward-rectifier Kir4.1 channels on the apical membranes of intermediate cells of the syncytium (Ando & Takeuchi, 1999; Marcus *et al.* 2002; Nin *et al.* 2008). We also confirmed that the low [K^+] in the IS, which is mandatory for the large K^+ diffusion potential, is maintained by K^+ uptake apparatus, Na^+,K^+-ATPases and Na^+,K^+,2Cl^--cotransporters (NKCCs) in the basolateral membranes of marginal cells, as had previously been suggested (Salt *et al.* 1987; Wangemann *et al.* 1995). KCNQ1/KCNE1 K^+ channels that occur in the apical surface of marginal cells (Sakagami *et al.* 1991; Sunose *et al.* 1994; Estévez *et al.* 2001) also produce a K^+ diffusion potential that contributes to the dynamics of the EP (Nin *et al.* 2008).

To further elucidate the mechanisms underlying the EP, we examined in this study the electrophysiological properties of another integral component of the lateral wall, the spiral ligament (Fig. 1*A*). Fibrocytes occupying this tissue constitute the basolateral surface of the syncytium (Fig. 1*B*). Although it is generally assumed that the fibrocytes' K^+ transport system is

critical for maintaining the EP (Konishi & Mendelsohn, 1970; Kuijpers & Bonting, 1970; Kusakari *et al.* 1978; Marcus *et al.* 1981; Shugyo *et al.* 1990; Wangemann, 2002; Higashiyama *et al.* 2003, 2010), the mechanism remains largely unexplored. We focused attention on the Na^+,K^+-ATPase abundantly expressed in fibrocytes, because this ion pump seems to play more important roles in the K^+ transport system of the ligament than other apparatus (Diaz *et al.* 2007). While monitoring the potential and $[K^+]$ in various compartments of the lateral wall, we perfused into scala tympani blockers of the Na^+,K^+-ATPase. The results constitute the first direct demonstration that K^+ transport driven by the fibrocytes' ATPase is essential for maintaining the electrochemical properties of the syncytium to form the positive ISP and EP.

Methods

General information

The experimental protocol was approved by the Animal Research Committees of Osaka University Graduate School of Medicine and Niigata University School of Medicine. The experiments were carried out under the supervision of the Committees and were performed in accordance with the Guidelines for Animal Experiments of Osaka University and Niigata University and the Japanese Animal Protection and Management Law.

Albino guinea pigs (200–400 g; SLC Inc., Hamamatsu, Japan) were first deeply anaesthetized I.P. with pentobarbital sodium (30 mg kg^{-1}; Nembutal, Abbott, IL, USA). To assess the depth of anaesthesia, toe pinch, corneal reflex and respiratory rate were used as a guide. When anaesthesia was not sufficient, pentobarbital sodium (5 mg kg^{-1}) was further given to the animals. Next, neuromuscular blockade was achieved with via an I.P. injection of vecuronium bromide (4 mg kg^{-1}), and the animals were artificially respirated for the electrophysiological experiments. Additional anaesthetic (10 mg kg^{-1}) was provided to the animals I.P. every 1–1.5 h (Ueno *et al.* 1982). Because neuromuscular blockade agents were used, during the experiments the depth of anaesthesia was monitored by fluctuations in heart rate. The animals were finally killed by an overdose of pentobarbital sodium (400 mg kg^{-1}).

Measurement of potential and aK^+

Using double-barrelled K^+-selective microelectrodes and a high input impedance differential amplifier/electrometer (FD223a; WPI, Sarasota, FL, USA), we measured simultaneously the potential and K^+ activity (aK^+) in the lateral wall and endolymph of the second cochlear turn. The experimental protocol largely followed that described in Nin *et al.* (2008). Electrodes were fabricated from double-barrelled borosilicate capillary glass (WPI) and a K^+ exchanger (IE190; WPI) was inserted into the salinized interior of one barrel. The K^+-selective barrel was backfilled with 150 mM KCl and the reference barrel was filled with 150 mM NaCl to avoid leakage influencing the K^+-selective electrode. Before every assay, the electrode sensitivity was first calibrated at 37°C with series of aqueous solutions containing (in mM) 15 KCl, 50 KCl and 150 KCl. In these experiments, we used only electrodes whose measured sensitivity profiles did not deviate from an ideal slope by more than 10% at any KCl concentration. Electrodes were calibrated at 37°C before and after each experiment by using reference solutions containing ([KCl]/[NaCl], in mM): 1.5/148.5, 5/145, 15/135, 50/100 and 150/0. The data were fit to a quadratic function that was then used to convert measured diffusion potentials into ionic activity (Supplemental Fig. 1).

The cochlea was exposed by a lateral approach (Kuijpers & Bonting, 1970; Plontke *et al.* 2008), and the electrode was driven through the lateral wall by a micromanipulator (MP-285; Sutter Instrument Company, Novato, CA, USA). An Ag–AgCl wire affixed to neck musculature served as a reference electrode. Slow drifts in voltage were typically less than 3 mV when measured with the pipette tip pulled back to the perilymph.

Perilymphatic perfusion of blockers

A thin tube (MicroFil; WPI), which was connected to a syringe containing the test solutions, was inserted into the scala tympani of the cochlea through a tiny fenestra that was made by a fine needle in the bony wall of the first cochlear turn. Perilymphatic perfusion of the solutions through the tube was then performed at a rate of 50 nl s^{-1} (Marcus *et al.* 1981) while the potential and aK^+ were monitored. The solutions were drained from the scala vestibuli through a small hole in the bony wall of the third cochlear turn. To perfuse the different solutions, the syringe was exchanged while the tube remained in the scala tympani. Ouabain (50 μM and 1 mM) was added to a control solution containing (in mM): 136.5 NaCl, 5.4 KCl, 1.8 $CaCl_2$, 0.53 $MgCl_2$ and 5.0 Hepes at pH 7.4. Strophanthidin (50 μM) was dissolved before use in DMSO, which was present in test solutions at a concentration of 0.05%. As reported previously (Kujawa *et al.* 1996; Suzuki *et al.* 2004), this solvent negligibly affected the EP and aK^+ of the endolymph (Supplemental Fig. 2).

Vascular perfusion of blockers

Vascular perfusion of the stria vascularis was performed at a rate of 1.5 ml min^{-1} through a polyethylene tube located in the left vertebral artery, from which capillaries extend

into the stria vascularis (Hibino *et al.* 1997). The blockers were dissolved in the aforementioned control solution.

Results

Effects of inhibiting fibrocyte Na^+,K^+-ATPase on the EP

The first series of experiments were conducted to evaluate our experimental technique and to confirm that inhibition of the Na^+,K^+-ATPase in the spiral ligament led to a loss of the EP. While measuring the EP and aK^+ with a double-barrelled electrode sensitive to both voltage and K^+, we perfused blockers of this K^+ pump into the scala tympani (Fig. 2 and Supplemental Fig. 3*A*). Of note, an ionic activity is an effective concentration of an ion, or in other words a measure of the fraction of the ions that are free and active and actually elicit a variety of chemical and biological phenomena including the diffusion potential monitored with the ion-selective electrode. An ionic activity is the product of the ion's concentration and its activity coefficient. Because the coefficient is variable and unmeasurable in intact cells and tissues, the value of aK^+ was measured and reported in this study.

In the example of Fig. 2*A*, we measured an aK^+ value of 3.7 mM in the perilymph. Upon advancing the electrode, the potential and aK^+ increased markedly and rapidly became stable, indicating that the electrode had entered the endolymph. The average EP and endolymphatic aK^+ under normal conditions were $+83.3 \pm 1.5$ mV and 103.5 ± 1.3 mM (mean ± SE, $n = 12$), respectively. During perilymphatic perfusion of ouabain (50 μM), an irreversible antagonist of Na^+,K^+-ATPases, the EP declined monotonically, stabilizing at a minimum of +8.0 mV after approximately 30 min; the aK^+ of the endolymph, by contrast, was relatively unaffected (Fig. 2*A*). Perfusing with this blocker for 40 min decreased the EP by 67.1 ± 6.6 mV ($n = 3$) (Table 1). More extreme effects were observed by perfusing 1 mM ouabain, which reduced the EP by 116.7 ± 3.7 mV ($n = 5$) (Fig. 2*B* and Table 1). In each of five experiments the potential fell to a minimum of roughly –20 to –35 mV. In addition, the endolymphatic aK^+ decreased gradually during the perfusion. These results accord with those reported in previous studies (Konishi & Mendelsohn, 1970; Kuijpers & Bonting, 1970; Sellick & Johnstone, 1974; Kusakari *et al.* 1978; Bosher, 1980; Marcus *et al.* 1981; Shugyo *et al.* 1990; Higashiyama *et al.* 2010), confirming that the blockers were perfused into the perilymph of the scala tympani. Moreover, perfusion of 50 μM strophanthidin, a reversible Na^+,K^+-ATPase blocker, reduced the EP by 73.0 ± 4.0 mV ($n = 4$) (Table 1 and Supplemental Fig. 3*A*).

In the spiral ligament of the lateral cochlear wall, the fibrocytes are the dominant cell type; they express Na^+,K^+-ATPases (Schulte & Adams, 1989; Schulte & Steel, 1994; Sakaguchi *et al.* 1998) and directly contact the perilymph (Fig. 1*B*). The pump in fibrocytes should therefore be a target of blockers applied to perilymph. Together with previous studies, the observations from Fig. 2 indicate that the Na^+,K^+-ATPase expressed in fibrocytes is crucial for establishing the EP.

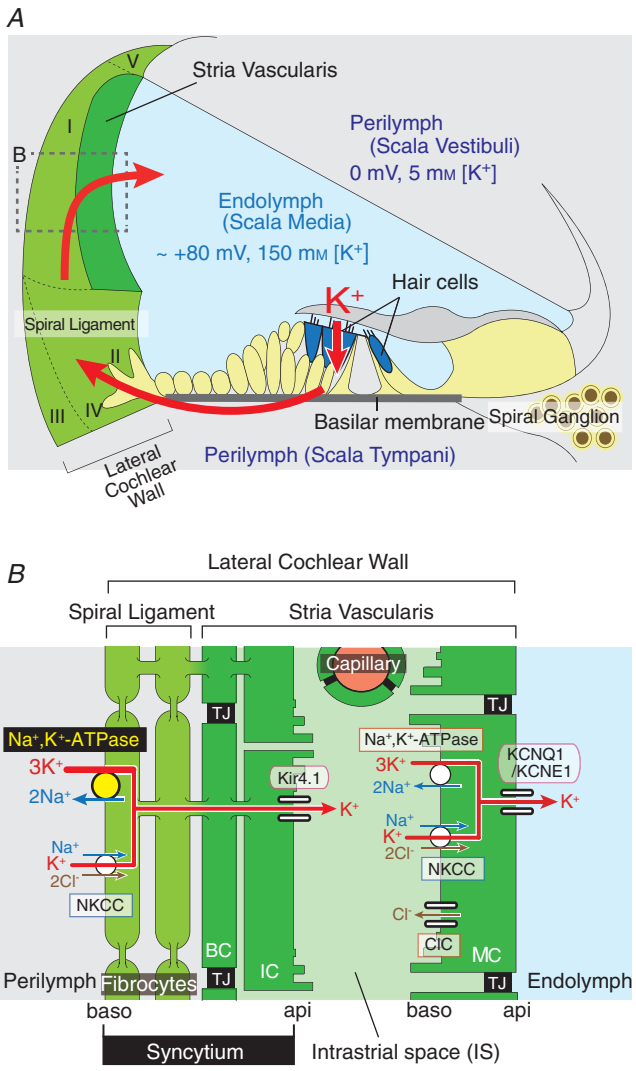

Figure 1. Structure of the cochlea and details of the lateral cochlear wall
A, schematic diagram of the cochlea. K^+ is transported from the endolymph to the perilymph, then back again to the endolymph through the lateral cochlear wall. The locations of the five types of fibrocyte are indicated by roman numerals. The potentials and K^+ concentrations of endolymph and perilymph are shown. *B*, an enlargement of the boxed region in *A*. Note that intermediate cells, basal cells and fibrocytes were interconnected by gap junctions and form an electrochemical 'syncytium' (Wangemann *et al.* 1995; Takeuchi & Ando, 1998; Takeuchi *et al.* 2000; Cohen-Salmon *et al.* 2007). The ion transport apparatus involved in the formation of the EP includes: NKCC, $Na^+,K^+,2Cl^-$-cotransporter; ClC-K, Cl^- channels ClC-K/barttin. Other abbreviations are: TJ, tight junction; IC, intermediate cell; BC, basal cell; api, apical; baso, basolateral. *A* and *B* are modified from figure 1 in Nin *et al.* (2008).

Electrochemical properties of the IS during inhibition of Na^+,K^+-ATPase

Two epithelial barriers and the IS in the lateral cochlear wall separate the endolymph of the scala media and the perilymph of the scala tympani (Fig. 1*B*). To further clarify the mechanism underlying the reduction of the EP caused by blocking the Na^+,K^+-ATPase in fibrocytes, we analysed the electrochemical properties of the IS. By advancing a double-barrelled, K^+-selective electrode from the perilymph into the stria vascularis, we were able to monitor the potential and aK^+ simultaneously while the scala tympani was perfused with blockers (Fig. 3).

Table 1. Effects of perilymphatic perfusion of Na^+,K^+-ATPase blockers on the EP

Blocker	ΔEP (mV)	*n*
Ouabain (50 μM)	67.1 ± 6.6	3
Ouabain (1 mM)	116.7 ± 3.7*	5
Strophanthidin (50 μM)	73.0 ± 4.0†	4

ΔEP, subtraction of initial EP from the minimum value that was detected at the end of the period of the perfusion. *Significantly different from any other values ($P < 0.05$). †Not significantly different from the value obtained during perfusion of 50 μM ouabain.

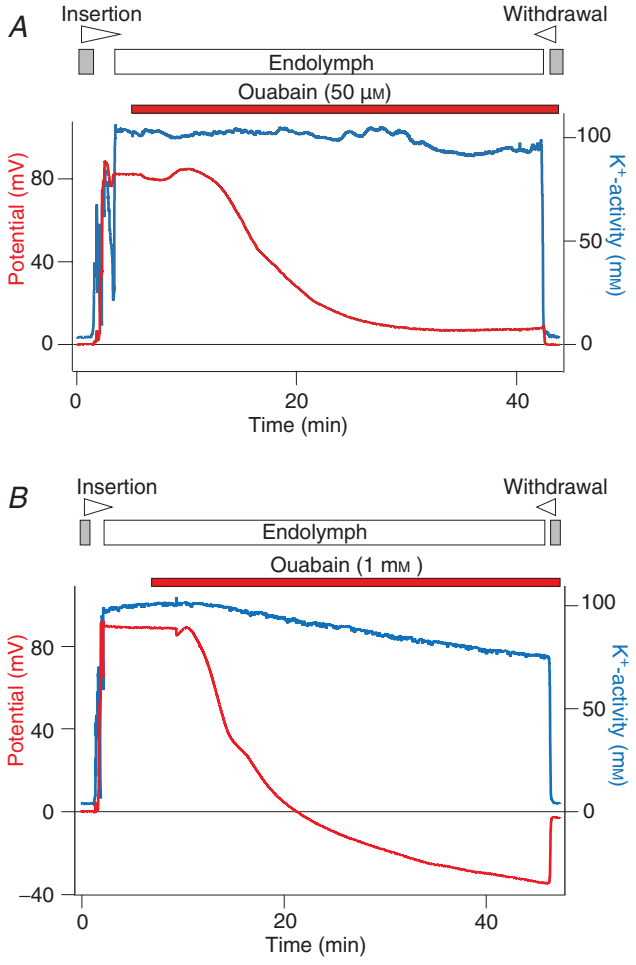

Figure 2. Effects of blocking fibrocyte Na^+,K^+-ATPase on the EP
A double-barrelled K^+-selective electrode, which simultaneously monitored potential and K^+ activity (aK^+), was advanced from the perilymph (grey bar above the traces) to the endolymph (open bar above the traces) to measure the EP. In this and subsequent recordings, the wedge at the top of each panel indicates the period during which the electrode was driven forward or backward through the tissue. The solution containing a blocker of Na^+,K^+-ATPase, ouabain at 50 μM (*A*) or 1 mM (*B*), was perfused into the perilymph of the scala tympani. The reagent was applied for the periods shown by the bars. In each experiment the electrode was finally retracted into the perilymph.

We first examined the effects of 50 μM ouabain (Fig. 3*A*). At the outset of the experiment, while the electrode was situated in the perilymph, aK^+ was 3.2 mM. Upon further insertion of the electrode, aK^+ fluctuated widely; peak values ranged from 32.0 to 71.5 mM (Fig. 3*A*, inset; see also Fig. 4*A*). This finding is consistent with the syncytium's property that we have described previously (Nin *et al.* 2008). Although in our previous study we found that the syncytium exhibited a potential of 0 to +4 mV (Nin *et al.* 2008), in this study, as shown in Fig. 3*A*, the potential typically ranged from 0 to +6.3 mV and was occasionally as high as +15.0 mV (see also Figs 4*A* and 5). In our earlier work, we additionally identified a region with a slight negative potential (–4 mV) and a moderate aK^+ (20 mM; Nin *et al.* 2008); we did not detect this in the present study. The inconsistencies could be due to variability in the animal colonies.

Upon entering the IS, we measured a low aK^+ value similar to that in the perilymph and a highly positive potential of +82.0 mV (Fig. 3*A*). Among 11 measurements the average aK^+ was 3.5 ± 0.2 mM and the average potential was +77.8 ± 1.2 mV. In the example shown in Fig. 3*A*, perilymphatic perfusion of 50 μM ouabain gradually reduced the ISP to +12.0 mV with little change in the aK^+ of the IS. The average of the ISP decrease in response to this blocker was 66.2 ± 2.5 mV ($n = 4$) (Table 2). Upon the electrode's entrance into endolymph, signalled by a rapid and prominent elevation of aK^+, the potential dropped by 3 mV (Fig. 3*A*). Similar results were observed in three other trials (Table 2).

In an earlier study we demonstrated that the ISP is primarily a K^+ diffusion potential that depends on a K^+ gradient across the apical surface of the syncytium (Nin *et al.* 2008), as had previously been suggested (Salt *et al.* 1987; Takeuchi *et al.* 2000). The ISP is described by the Nernst equation

$$\mathrm{ISP} = V_{\mathrm{Syn}} + \frac{RT}{F} \ln\left(\frac{aK^+_{\mathrm{i(Syn)}}}{aK^+_{\mathrm{IS}}}\right), \qquad (1)$$

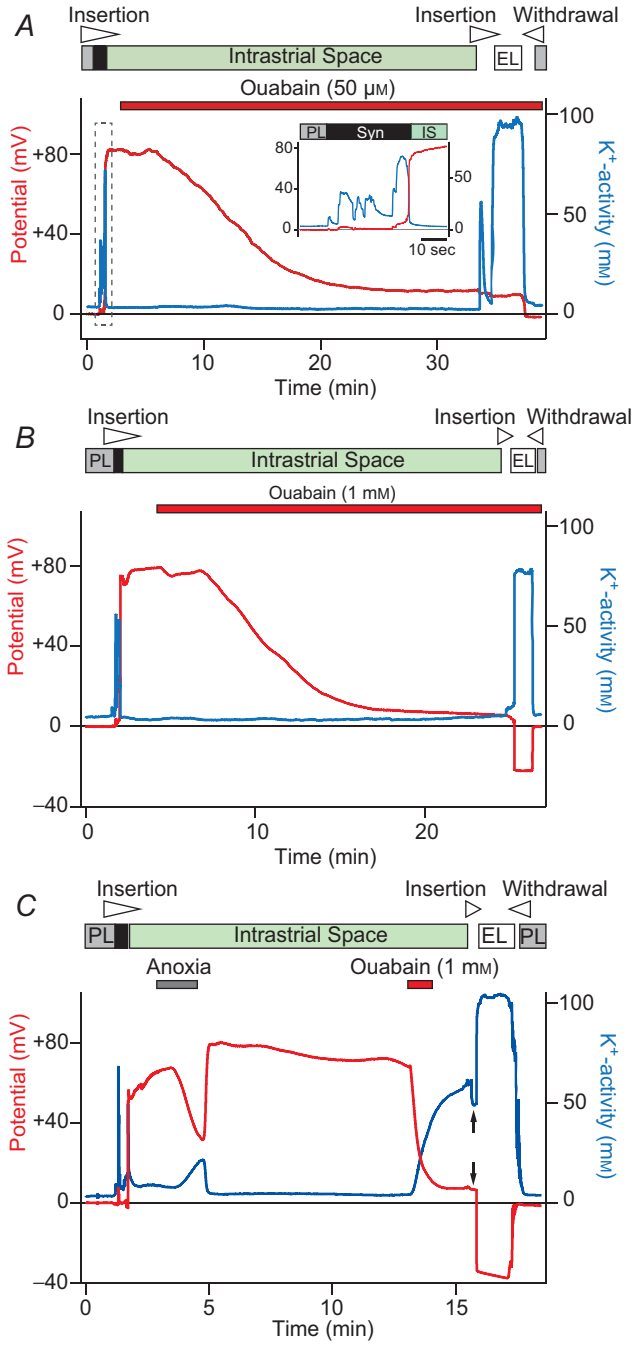

Figure 3. Properties of the IS during blockage of Na^+,K^+-ATPase in the lateral wall
The potential (red) and aK^+ (blue) of compartments of the lateral cochlear wall were recorded with a double-barrelled K^+-selective electrode advanced from the perilymph (PL; grey bars above the traces) to the endolymph (EL; open bars above the traces). Before encountering the intrastrial space (IS), we detected a region of the syncytium (Syn, black bars above the traces). While the electrode was held in the IS (green bars above the traces), blockers were applied to particular compartments of the cochlea (see below). The electrode was finally advanced until it entered the endolymph, which was indicated by a sudden increase in the aK^+. *A* and *B*, the effect of perilymphatic perfusion of ouabain at 50 μM (*A*) or 1 mM (*B*). In *A*, the area surrounded by the broken square is displayed in the inset with an expanded time scale. *C*, while the electrode was placed in the IS, the animal was subjected to anoxia. After reoxygenation, 1 mM ouabain was injected into a vertebral artery, the origin of the capillaries in the stria vascularis. Arrows point to the inside of marginal cells, in which the aK^+ was 48.0 mM and the potential was similar to the ISP.

in which V_{Syn} and $aK^+_{i(Syn)}$ are the potential and intracellular K^+ activity of the syncytium, aK^+_{IS} is the extracellular K^+ activity of the IS, and R, T and F are the ideal gas constant, temperature and Faraday constant (Nin *et al.* 2008; Hibino *et al.* 2010). Under normal conditions, V_{Syn} is low (Fig. 3*A*; see also Figs 4*A* and 5), indicating that its contribution to the EP is modest. Because inhibition of the fibrocytes' Na^+,K^+-ATPase by 50 μM ouabain had little effect on aK^+_{IS} in the present study (Fig. 3*A*), this blocker probably reduced the ISP by decreasing $aK^+_{i(Syn)}$ or V_{Syn}.

Marginal cells are the sole boundary between the IS and endolymph (Fig. 1*B*). The EP might therefore represent the sum of the ISP and the potential difference across the marginal cells (Takeuchi *et al.* 2000). The basolateral surface of the marginal cells probably expresses little K^+ and Na^+ conductance (Shindo *et al.* 1992; Takeuchi *et al.* 1995). Furthermore, although this membrane exhibits Cl^- conductance (Takeuchi *et al.* 1995), Cl^- activity in the IS is similar to that inside the marginal cells (Nin *et al.* 2012). As demonstrated in our early studies, the potential inside the marginal cells is therefore nearly equal to the ISP (Nin *et al.* 2008, 2012). At the apical surfaces of the marginal cells, the K^+ permeability significantly exceeds the Na^+ and Cl^- permeabilities (Takeuchi *et al.* 1992; Wangemann, 1995; Shen & Marcus, 1998). The EP would therefore depend primarily on the potential of the marginal cells and a K^+ diffusion potential across the apical surface of marginal cells:

$$\mathrm{EP} = V_{\mathrm{MC}} + \frac{RT}{F}\ln\left(\frac{aK^+_{i(\mathrm{MC})}}{aK^+_{\mathrm{EL}}}\right), \qquad (2)$$

in which V_{MC} is the potential of the marginal cells with reference to the perilymph and $aK^+_{i(MC)}$ and aK^+_{EL} are the K^+ activities inside the marginal cells and in the endolymph. Supporting this formulation, we previously showed that the measured EP closely matched the EP predicted by eqn (2) under various conditions, using measured values of V_{MC}, $aK^+_{i(MC)}$ and aK^+_{EL} (Nin *et al.* 2008). Because V_{MC} is similar to the ISP (see above), eqn (2) can be modified with eqn (1) as follows

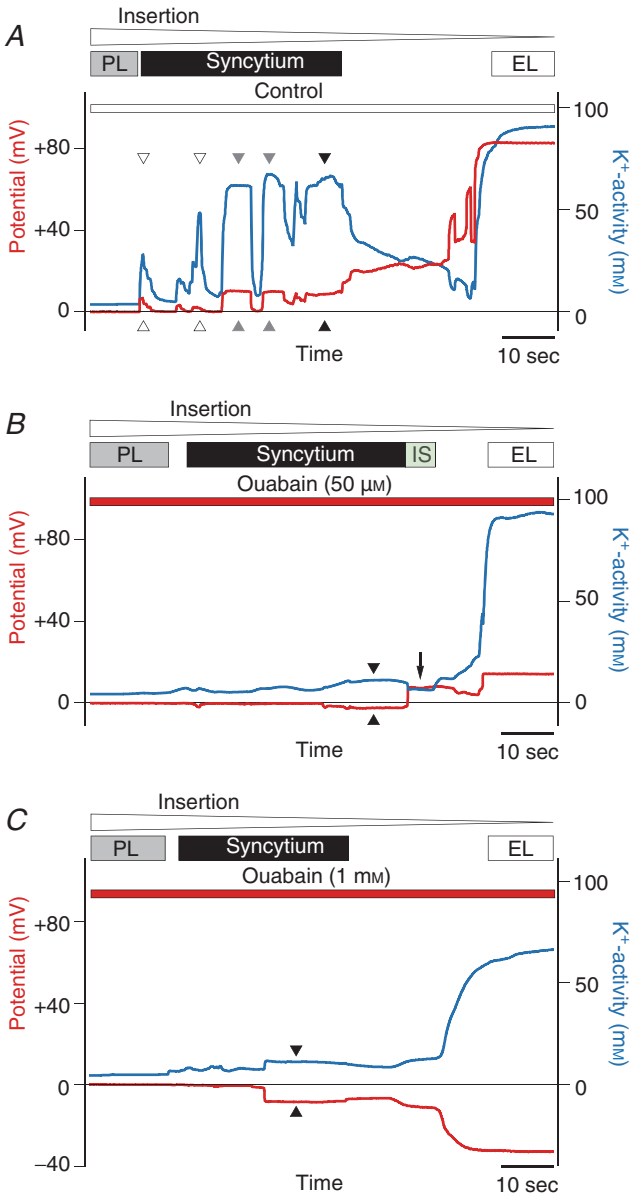

Figure 4. Analysis of properties within the syncytium
Solutions containing no blocker (*A*), 50 μM ouabain (*B*) or 1 mM ouabain (*C*) were first perfused into the scala tympani for 50 min. The K$^+$-selective electrode was subsequently advanced from the perilymph (PL; grey bars above the traces) to the endolymph (EL; open bars above the traces) to examine the properties of the syncytium (black bars above the traces) while the perfusates were being applied. In *A*, on passage through the syncytium region, the electrode detected five compartments showing an elevated aK$^+$ and a slightly positive potential. The properties of three compartments indicated by grey and filled arrowheads were stably measured whereas those of two compartments marked by open arrowheads showed a spike-like appearance. When examining the cochleae perfused with ouabain at 50 μM (*B*) or at 1 mM (*C*), we could not clearly observe compartments other than the IS (arrow in *B*) and the endolymph. In *A*, *B* and *C*, the aK$^+$ and the potential of the region that neighboured the IS or the endolymph (filled arrowheads) were taken to characterize the effect of the blockers on the syncytium's properties in Fig. 5 (see text).

(Hibino *et al.* 2010):

$$\begin{aligned} \mathrm{EP} &= \mathrm{ISP} + \frac{RT}{F}\ln\left(\frac{a\mathrm{K}^+_{\mathrm{i(MC)}}}{a\mathrm{K}^+_{\mathrm{EL}}}\right) \\ &= V_{\mathrm{Syn}} + \frac{RT}{F}\ln\left(\frac{a\mathrm{K}^+_{\mathrm{i(Syn)}}}{a\mathrm{K}^+_{\mathrm{IS}}}\right) \\ &\quad + \frac{RT}{F}\ln\left(\frac{a\mathrm{K}^+_{\mathrm{i(MC)}}}{a\mathrm{K}^+_{\mathrm{EL}}}\right). \end{aligned} \tag{3}$$

Under physiological conditions, aK$^+_{\mathrm{EL}}$ (95–110 mM) exceeds aK$^+_{\mathrm{i(MC)}}$ (80 mM), which imposes a K$^+$ diffusion potential of up to 15 mV through KCNQ1/KCNE1 channels in the apical surfaces of the marginal cells (Fig. 1*B*; Melichar & Syka, 1987; Offner, 1987; Nin *et al.* 2008). In the present study, during the perfusion of 50 μM ouabain the potential difference across the marginal cells, which resembles the potential difference across the apical surfaces of marginal cells (see above), was small, 5.6 ± 1.1 mV (n = 4) (Fig. 3*A* and Table 2). We also found that in this condition aK$^+_{\mathrm{EL}}$ was nearly constant (Fig. 2*A*). These two observations imply that the reduction of the EP (Fig. 2*A*) stems primarily from a decrease in the ISP, with a negligible change in aK$^+_{\mathrm{i(MC)}}$ (eqn 3). Similarly, when 50 μM strophanthidin was perfused into the perilymph, the ISP was reduced by 67.9 ± 4.1 mV and exceeded the

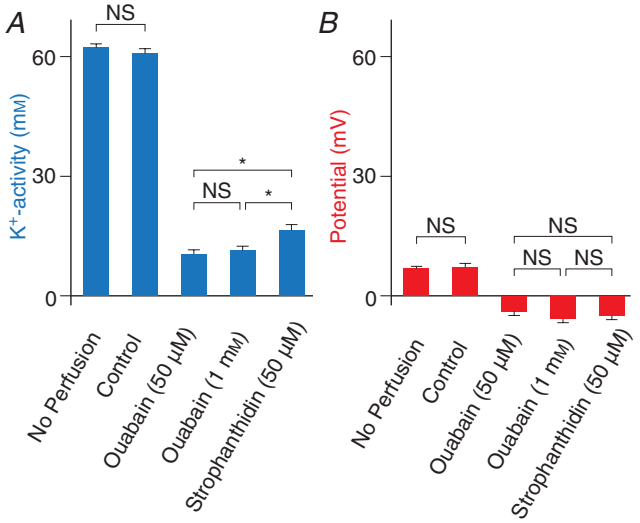

Figure 5. Effects of blocking the fibrocytes' Na$^+$,K$^+$-ATPase on the syncytium's aK$^+$ and potential
Displayed are syncytium's properties that were characterized as described in the text, on the basis of the experimental results of Fig. 4 and Supplemental Fig. 3*C*, for cochleae treated with no perfusate (n = 40), or perilymphatically perfused with control solution (n = 6), 50 μM ouabain (n = 8), 1 mM ouabain (n = 10), and 50 μM strophanthidin (n = 11). Averages and SE are shown. *Significantly different ($P < 0.01$). NS, not significantly different ($P > 0.05$).

Table 2. Effects of perilymphatic perfusion of Na^+,K^+-ATPase blockers on the ISP

Blocker	ΔISP (mV)	ISP – EP (mV)	*n*
Ouabain (50 μM)	66.2 ± 2.5	5.6 ± 1.1	4
Ouabain (1 mM)	75.8 ± 2.1†	24.2 ± 3.5*	3
Strophanthidin (50 μM)	67.9 ± 4.1†	8.6 ± 5.2‡	4

ΔISP, subtraction of initial ISP from the minimum value that was detected at the end of the period of the perfusion. †Not significantly different from any other values. *Significantly different from any other values ($P < 0.05$). ‡Not significantly different from the value obtained during perfusion of 50 μM ouabain.

EP by 8.6 ± 5.2 mV in the steady state ($n = 4$) (Table 2 and Supplemental Fig. 3*B*). These values were not significantly different from those recorded during perfusion of 50 μM ouabain (Table 2). Moreover, as in the case of 50 μM ouabain, 50 μM strophanthidin barely affected the value of aK^+_{IS} (Supplemental Fig. 3*B*). Perilymphatic perfusion of 1 mM ouabain also had little effect on aK^+_{IS} and decreased the ISP by 75.8 ± 2.1 mV ($n = 3$) in a manner similar to ouabain at 50 μM (Fig. 3*B* and Table 2). Therefore, application of 50 μM strophanthidin or 1 mM ouabain seems to impair the ISP by affecting $aK^+_{i(Syn)}$ or V_{Syn} (eqns 1 and 3), as predicted in the case of 50 μM ouabain. However, when 1 mM ouabain was perfused, the ISP greatly exceeded the EP in the steady state, providing across the marginal cells a difference of 24.2 ± 3.5 mV ($n = 3$) (Fig. 3*B*). This value significantly exceeds the difference elicited by the perfusion of 50 μM ouabain or 50 μM strophanthidin (Table 2). These results might account for the observation that perfusion of 1 mM ouabain reduced the EP more strongly than that of 50 μM ouabain or 50 μM strophanthidin (Table 1), because the three perturbations decreased the ISP in a similar manner (Table 2 and eqn 3). Ouabain at the higher concentration might additionally alter the properties of other cell types, such as marginal cells, that could significantly influence the EP (eqn 3; see Discussion). Nevertheless, even in the case of 1 mM ouabain, because the reduction of the ISP greatly exceeded the potential difference across marginal cells (75.8 ± 2.1 *vs.* 24.2 ± 3.5 mV, Table 2), it is clear that the decline of the EP stemmed mainly from the change of the syncytium's electrochemical properties.

Anoxia and vascular perfusion of 1 mM ouabain, both of which block Na^+,K^+-ATPase expressed at the basolateral surface of marginal cells, decreased the ISP and increased the aK^+_{IS} (Fig. 3*C*) as we previously found (Nin *et al.* 2008). The increase of aK^+_{IS} is a major factor that underlies the reduction of the ISP, as $aK^+_{i(Syn)}$ probably does not change (Nin *et al.* 2008; eqn 1). As depicted in Fig. 3*C*, during blockage of the marginal cells' Na^+,K^+-ATPase by 1 mM ouabain, the electrode was advanced farther. Before encountering the endolymph, we detected the marginal cells' cytoplasm showing a potential similar to the ISP and an aK^+ of 48 mM that was prominently lower than aK^+_{IS} and aK^+_{EL} (Fig. 3*C*, arrow). Under this condition, $aK^+_{i(MC)}$, which is approximately 80 mM under physiological conditions, was probably reduced by ouabain (Nin *et al.* 2008). aK^+_{EL} seemed to be constant even when the marginal cells' Na^+,K^+-ATPase was inhibited (Nin *et al.* 2008). Therefore, the change in $aK^+_{i(MC)}$ might enhance the K^+ diffusion potential across the apical surfaces of marginal cells, providing a prominent potential difference across these cells (eqns 2 and 3; Fig. 3*C* and Table 2; Nin *et al.* 2008). Indeed, the electrode recorded a large reduction of the potential (41 mV) when it was advanced beyond the marginal cells and into the endolymph (Fig. 3*C*). Taking these data together, it is clear that the mechanism underlying the reduction of the EP by the perilymphatic perfusion of the blockers differs from that induced by anoxia and by the vascular perfusion of ouabain (see Fig. 3 and Supplemental Fig. 3*B*).

Role of fibrocyte K^+ transport in generation of the EP

Analysis of the IS (Fig. 3) suggests strongly that suppression of the ISP by perilymphatic perfusion of the blockers is caused by a change of $aK^+_{i(Syn)}$ or V_{Syn}. To determine which factor was responsible, we examined the syncytium with a K^+-selective electrode. Fibrocytes, the major constituents of the syncytium, have little cytoplasm and highly invaginated membranes (Takahashi & Kimura, 1970; Kikuchi *et al.* 1995; Spicer & Schulte, 1996, 2002). These features complicate insertion of an electrode in the syncytium. Among 24 experiments, the electrode seemed to enter and remain inside the syncytium, but the measurement became unstable after several minutes. At such short delay, the blockers cannot sufficiently suppress the EP and the ISP (Figs 2 and 3). We therefore took an alternative approach: the solution in the presence or absence of the blockers was first perfused into the perilymph for 50 min. Thereafter, the perfusate continued to be applied and the K^+-selective electrode was driven from the perilymph toward the endolymph across the lateral cochlear wall (1.5 μm s^{-1}) to examine the syncytium (Figs 4 and 5).

Figure 4*A* shows at an expanded time scale the electrochemical properties of the lateral wall during perfusion of a control solution that contained no blocker. Within the syncytium region, the electrode clearly encountered five compartments other than the perilymph. When the electrode was inserted into each of the three compartments closer to the endolymph than the other two compartments, the aK^+ abruptly increased and reached a plateau of 62.0–67.6 mM (Fig. 4*A*, grey and filled arrowheads). The potential also followed a similar course, reaching a maximum of +8.9 to +10.2 mV. These

observations indicate that the electrode had entered the cells constituting the syncytium and steadily monitored the electrochemical properties. By contrast, when the electrode passed through the other two compartments, aK^+ and the potential displayed spike-like variations with peak values of 28.3–48.6 mM and +1.9 to +6.3 mV, respectively (Fig. 4*A*, open arrowheads). This could have occurred if the electrode penetrated the invaginated processes of the fibrocytes, injured the cells or was transiently advanced into the cells' small volume of cytoplasm. In support of these possibilities, aK^+ in the former three compartments (>60 mM) was significantly higher than aK^+ in the latter two compartments (<50 mM). In the assay depicted in Fig. 4*A*, the IS was not clearly detected before the endolymph; this result was sometimes observed in our previous studies (Nin *et al.* 2008).

Within the syncytium region in each of the six cochleae perfused with the control solution, we observed the compartment other than the perilymph multiple times (2–5) and never recorded a negative potential. The compartment neighbouring the IS or the endolymph exhibited the highest aK^+ (58.6–60.4 mM) in five cochleae, and it also exhibited aK^+ similar to the highest value (66.7 *vs.* 67.6 mM) in one case. In addition, aK^+ and the potential in this compartment were always stable ($n = 6$). Similar results were obtained when the cochleae treated without perfusate were assayed ($n = 40$). We conclude that, in each experiment, this compartment probably represents the inside of the syncytium (Fig. 4*A*, filled arrowhead). These measurements were therefore used to characterize the electrochemical properties of the syncytium (Fig. 5). The mean values of aK^+ and potential measured in cochleae that were perfused with a control solution were 60.9 ± 1.2 mM and +7.2 ± 0.9 mV ($n = 6$); these values are not significantly different from those recorded in the cochleae that were not perfused (aK^+ 62.3 ± 1.0 mM, potential +6.9 ± 0.5 mV, $n = 40$; Fig. 5). The compartment that was observed adjacent to the IS or the endolymph may correspond to the inside of basal cells or of intermediate cells for the following reasons. Fibrocytes are scattered throughout the spiral ligament and in some cases might not be encountered by the electrode. Additionally, basal cells form a continuous monolayer and many intermediate cells overlie this layer (Fig. 1*B*); the electrode could enter either of these two cell types in every trial.

We next examined the lateral wall during perfusion with 50 μM ouabain (Fig. 4*B*). On insertion of the electrode but before encountering the endolymph, we observed the IS exhibiting an aK^+ similar to that measured in the perilymph and a potential of +7.5 mV (filled arrow) but could not clearly detect other compartments. It strongly suggests that $aK^+_{i(Syn)}$ was low in this condition. We examined 10 cochleae and, to estimate the properties of the syncytium, averaged the aK^+ and potential of the regions observed adjacent to the IS or the endolymph (filled arrowhead in Fig. 4*B*). The mean values were 10.4 ± 1.2 mM and −3.9 ± 0.8 mV, respectively (Fig. 5). These observations imply that the inhibition of fibrocytes' Na^+,K^+-ATPase by the perilymphatic perfusion of 50 μM ouabain greatly reduces aK^+ and modestly hyperpolarizes the potential in the syncytium. Reduction of the aK^+ probably diminishes the K^+ gradient across the apical surface of the syncytium, thereby suppressing the ISP (see eqn 1 and Fig. 6). This mechanism might account for the decline in the EP because, in the presence of 50 μM ouabain, the potential difference across the marginal cells is small and relatively unaffected (Fig. 3*A*, Table 2, and eqn 3). Hyperpolarization of the syncytium is also low, roughly 11 mV (Fig. 5*B*), and thereby modestly contributes to the change of the EP (eqn 3). The marked reduction of $aK^+_{i(Syn)}$ by ouabain strongly supports the hypothesis that active K^+ transport occurs across the fibrocytes' membranes *in vivo* as expected. Similar effects were observed during perfusion with 1 mM ouabain (Fig. 4*C*); the average aK^+ and potential in the syncytium were 11.3 ± 1.2 mM and −5.8 ± 1.2 mV ($n = 8$) (Fig. 5). These values were not significantly different from the results obtained during perfusion of 50 μM ouabain (Fig. 5). Therefore, the fibrocytes' Na^+,K^+-ATPase seemed to be fully blocked by ouabain at a concentration as low as 50 μM. Perfusion of 50 μM strophanthidin similarly hyperpolarized the potential (−5.0 ± 0.8 mV) but reduced the aK^+ to lesser extent (16.5 ± 1.5 mM; $n = 11$) (Fig. 5 and Supplemental Fig. 3*C*). This blocker nevertheless suppressed the ISP to the same extent as 50 μM ouabain (Supplemental Fig. 3*B*; see also Figs 3*A* and 3*B* and Table 2).

Discussion

The spiral ligament has been thought to be involved in formation of the EP (Konishi & Mendelsohn, 1970; Kuijpers & Bonting, 1970; Kusakari *et al.* 1978; Marcus *et al.* 1981; Komune *et al.* 1985; Shugyo *et al.* 1990; Minowa *et al.* 1999; Kikuchi *et al.* 2000; Wangemann, 2002; Higashiyama *et al.* 2003, 2010). Fibrocytes express several types of K^+ transport apparatus that might participate in the flow of K^+ across the ligament, including Na^+,K^+-ATPase, NKCC type 1 (NKCC1), K^+,Cl^--cotranspoter and H^+,K^+-ATPase (Schulte & Adams, 1989; Schulte & Steel, 1994; Spicer & Schulte, 1996; Crouch *et al.* 1997; Xia *et al.* 1999; Boettger *et al.* 2003; Shibata *et al.* 2006). Of these apparatus, Na^+,K^+-ATPase and NKCC1 have been most extensively analysed using electrophysiological techniques (Konishi & Mendelsohn, 1970; Kuijpers & Bonting, 1970; Sellick & Johnstone, 1974; Kusakari *et al.* 1978; Marcus *et al.* 1981; Komune *et al.* 1985; Shugyo *et al.* 1990; Flagella *et al.* 1999; Higashiyama *et al.* 2003, 2010). Recently, progressive hearing loss and impairment of the EP have been detected in heterozygotic

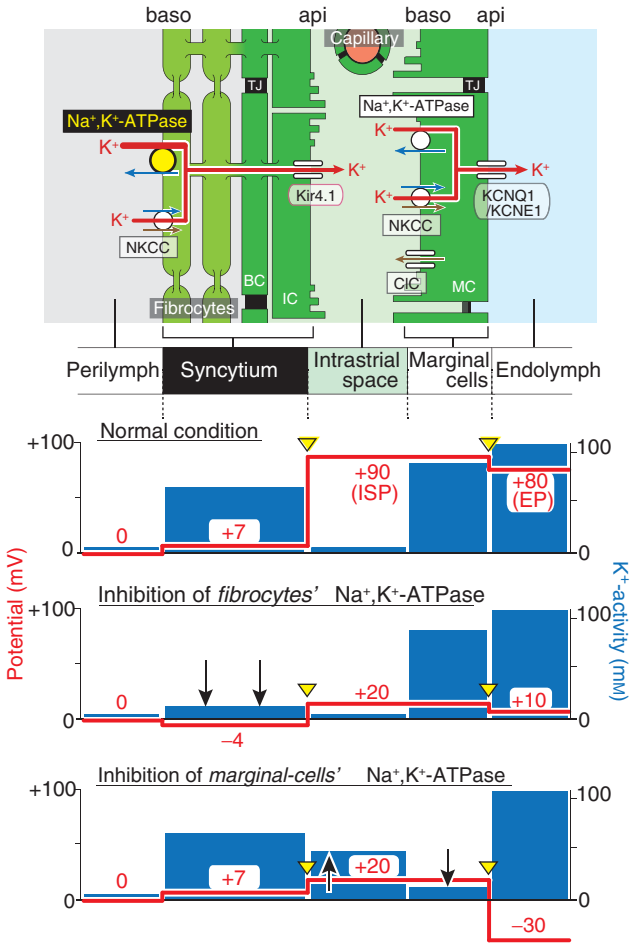

Figure 6. Summary of the electrochemical milieu of the lateral cochlear wall.
Top, the structure of the lateral wall and K^+ transport apparatus involved in the formation of the EP. The other panels display the predicted potential and aK^+ in each compartment under normal condition (second panel) and during inhibition of Na^+,K^+-ATPase in fibrocytes by perilymphatic perfusion of 50 μM ouabain (third panel) and that in marginal cells by vascular perfusion of 1 mM ouabain or anoxia (fourth panel). Arrowheads filled with yellow point to the membrane compartments in which a K^+ diffusion potential occurs. Upward and downward arrows show increases and decreases of aK^+ as compared to those in the normal condition. Of note, in the second condition (third panel), the aK^+ of the syncytium decreases whereas the aK^+ of the IS remains constant. This change diminishes the K^+ diffusion potential across the apical surface of the syncytium and, considering that potential difference across the marginal cells remains unchanged, is primarily responsible for reduction of the ISP and the EP. In contrast, the third condition (fourth panel) not only increases the aK^+ of the IS, which reduces the ISP, but also decreases the aK^+ within the marginal cells, which enlarges the K^+ diffusion potential across their apical surface. These two elements contribute to impairment of the EP. NKCC, $Na^+,K^+,2Cl^-$-cotransporter; ClC, Cl^- channels ClC-K/barttin; MC, marginal cell; IC, intermediate cell; BC, basal cell; IS, intrastrial space; TJ, tight junction; api, apical; baso, basolateral.

α_1- and α_2-Na^+,K^+-ATPase$^{+/-}$ mice, which are expected to experience a reduced activity of fibrocyte ATPase in the cochlea, as well as in NKCC1$^{+/-}$ animals (Diaz *et al.* 2007). This and previous studies suggest two things: first, in the fibrocytes the active K^+ transport may occur and be driven by the K^+ uptake apparatus; and second, the K^+ transport would contribute to the EP. *In vivo* experiments that examine electrochemical properties of the lateral wall during blockage of the apparatus could provide evidence that supports these hypotheses, but have heretofore not been performed. We therefore examined the lateral wall with K^+-selective electrodes. As for the aforementioned mutant animals, elevation of the hearing threshold occurred earlier in the α_1- and α_2-Na^+,K^+-ATPase$^{+/-}$ mice than in the NKCC1$^{+/-}$ mice during development. This implies primacy of Na^+,K^+-ATPase over NKCC1 in the K^+ transport system of fibrocytes (Diaz *et al.* 2007). Additionally, it was difficult to measure the narrow spaces of the IS and syncytium with an electrode. Therefore, in the present study we have focused on one transport process, the Na^+,K^+-ATPase, to examine the fibrocytes' K^+ transport and its relevance to the EP.

We demonstrated that perilymphatic perfusion of 50 μM ouabain decreases $aK^+_{i(Syn)}$ in living guinea pigs (Figs 4 and 5). This result may support a previous finding that the K^+ content of the lyophilized spiral ligament, measured by helium-glow photometry, declined during perilymphatic perfusion of ouabain (Marcus *et al.* 1981). Because ouabain had little effect on aK^+_{IS} (Figs 3*A* and 6), it diminished the K^+ gradient and thus the K^+ diffusion potential across the apical surface of the syncytium (eqn 1). This effect was largely responsible for reducing the ISP, because the syncytium was only moderately hyperpolarized (Figs 5 and 6; eqn 1). Furthermore, perfusion of 50 μM ouabain negligibly or only modestly changed the potential difference across the marginal cells (Figs 3*A* and 6; Table 2). These results imply that the decline of the EP is due primarily to a decrease of $aK^+_{i(Syn)}$ (eqn 3). Interestingly, perfusion of 1 mM ouabain induced across the marginal cells a large potential difference, which would significantly contribute to the reduction of the EP to negative values (Fig. 3*A* and Table 2). Although the mechanism that establishes the potential difference remains uncertain, it is possible that ouabain reaches marginal cells through an alternative pathway and modulates ionic properties within these cells. Alternatively, ouabain might induce a negative EP by affecting the transporter in other epithelial cells that are involved in maintenance of the EP. Nevertheless, because the reduction of the ISP greatly exceeds the marginal cell's potential difference (Table 2), the decline of the EP during the perfusion of 1 mM ouabain also stems primarily from the decrease of $aK^+_{i(Syn)}$ (eqn 3). Taken together, the results indicate that fibrocytes use the Na^+,K^+-ATPase to take up K^+ from the perilymph and thus maintain high

$aK^+_{i(Syn)}$, which is essential for the K^+ diffusion potential underlying the highly positive ISP and EP (Fig. 6). These observations provide the first *in vivo* evidence for active K^+ transport through fibrocytes and elucidate the mechanism of its contribution to the formation of the EP. This local K^+ transport could also mediate the unidirectional K^+ circulation through a pathway comprising perilymph, the lateral wall, endolymph and hair cells (Fig. 1). Strophanthidin at 50 μM reduces the ISP and the EP by a process similar to 50 μM ouabain, although strophanthidin appears to have an additional effect on the syncytium (see below). The mechanism underlying the reduction of the EP by anoxia and by vascularly perfused ouabain, however, is clearly different. These perturbations should block Na^+,K^+-ATPase on the basolateral surfaces of marginal cells because the capillaries in the stria vascularis form the densest network in the lateral wall (Slepecky, 1996). During anoxia or vascular perfusion of ouabain, the aK^+_{IS} increases markedly (Figs 3*C* and 6) as previously reported (Nin *et al.* 2008). The alteration diminishes the K^+ gradient across the apical surface of the syncytium because $aK^+_{i(Syn)}$ was probably unchanged (Nin *et al.* 2008; Fig. 6). The K^+ diffusion potential eventually decreases and the ISP declines (eqn 1). Simultaneously, ouabain and anoxia reduce $aK^+_{i(MC)}$ with little effect on aK^+_{EL}, causing the K^+ diffusion potential across the apical surface of marginal cells to enlarge (Fig. 3*C*; Nin *et al.* 2008). Due to the augmented potential difference across the marginal cells and the reduced ISP, the EP is largely impaired and becomes negative (eqn 3 and Fig. 6). Note that our previous study (Nin *et al.* 2008) quantitatively verified all the above processes by comparing the measured ISP and EP to those calculated by eqns (1) and (3) with the measured values of aK^+ in various compartments.

Under physiological conditions, V_{Syn} is slightly positive relative to the potential of the perilymph (Figs 4, 5 and 6), which permits the K^+ diffusion potential across the apical surface of the syncytium to form the highly positive ISP (Nin *et al.* 2008). The mechanism that sustains this electrical property of the syncytium remains elusive. Although $aK^+_{i(Syn)}$ declined markedly during perilymphatic perfusion of ouabain and strophanthidin, V_{Syn} was only modestly more negative and never more positive (Figs 4 and 5), suggesting that fibrocyte membranes express little K^+ permeability. Immunolabeling of ClC-K Cl^- channels has been detected in type II and IV fibrocytes (Qu *et al.* 2006). This has not been observed in other studies (Estévez *et al.* 2001; Sage & Marcus, 2001; Rickheit *et al.* 2008) but Cl^- conductance has been recorded in cultured fibrocytes (Maehara *et al.* 2003; Qu *et al.* 2006, 2007). Even if functional Cl^- channels are expressed in native fibrocytes, they might not be responsible for establishing the syncytium's characteristics: under physiological conditions, because $[Cl^-]$ seems to be higher in perilymph than within the syncytium (Ikeda & Morizono, 1989; Nin *et al.* 2012), a Cl^- conductance could hyperpolarize the fibrocytes with reference to the perilymph. Alternatively, if fibrocytes express non-selective cation channels and the cation concentration of the perilymph is higher than that inside the syncytium, then the syncytium's potential could be measured as positive. When Na^+,K^+-ATPase is blocked, the cation concentration inside the syncytium would increase and exceed that of the perilymph. This could subsequently allow non-selective cation channels to hyperpolarize the syncytium, an effect that we observed in the present study (Figs 4*B* and 5).

Although strophanthidin at 50 μM reduced the ISP and V_{Syn} as much as ouabain at all concentrations (Table 2), the effect of strophanthidin on $aK^+_{i(Syn)}$ was less prominent (Fig. 5 and Supplemental Fig. 3*C*). This inconsistency might indicate that strophanthidin, which is permeable through the membranes to some extent (Garner, 2002), affects ion transport mechanisms other than Na^+,K^+-ATPase on the apical surface of the syncytium and modulates ionic concentrations inside the syncytium or ionic permeabilities on this membrane compartment. Future studies should reveal ion transport mechanisms that control the milieu of the syncytium and its pharmacological properties.

References

Ando M & Takeuchi S (1999). Immunological identification of an inward rectifier K^+ channel (Kir4.1) in the intermediate cell (melanocyte) of the cochlear stria vascularis of gerbils and rats. *Cell Tissue Res* **298**, 179–183.

Boettger T, Rust MB, Maier H, Seidenbecher T, Schweizer M, Keating DJ, Faulhaber J, Ehmke H, Pfeffer C, Scheel O, Lemcke B, Horst J, Leuwer R, Pape HC, Volkl H, Hubner CA & Jentsch TJ (2003). Loss of K-Cl co-transporter KCC3 causes deafness, neurodegeneration and reduced seizure threshold. *EMBO J* **22**, 5422–5434.

Bosher S (1980). The effects of inhibition of the strial Na^+-K^+-activated ATPase by perilymphatic ouabain in the guinea pig. *Acta Otolaryngol* **90**, 219–229.

Cohen-Salmon M, Regnault B, Cayet N, Caille D, Demuth K, Hardelin JP, Janel N, Meda P & Petit C (2007). Connexin30 deficiency causes instrastrial fluid-blood barrier disruption within the cochlear stria vascularis. *Proc Natl Acad Sci U S A* **104**, 6229–6234.

Crouch JJ, Sakaguchi N, Lytle C & Schulte BA (1997). Immunohistochemical localization of the Na-K-Cl co-transporter (NKCC1) in the gerbil inner ear. *J Histochem Cytochem* **45**, 773–778.

Diaz RC, Vazquez AE, Dou H, Wei D, Cardell EL, Lingrel J, Shull GE, Doyle KJ & Yamoah EN (2007). Conservation of hearing by simultaneous mutation of Na,K-ATPase and NKCC1. *J Assoc Res Otolaryngol* **8**, 422–434.

Estévez R, Boettger T, Stein V, Birkenhäger R, Otto E, Hildebrandt F & Jentsch TJ (2001). Barttin is a Cl^- channel β-subunit crucial for renal Cl-reabsorption and inner ear K^+ secretion. *Nature* **414**, 558–561.

Flagella M, Clarke LL, Miller ML, Erway LC, Giannella RA, Andringa A, Gawenis LR, Kramer J, Duffy JJ, Doetschman T, Lorenz JN, Yamoah EN, Cardell EL & Shull GE (1999). Mice lacking the basolateral Na-K-2Cl cotransporter have impaired epithelial chloride secretion and are profoundly deaf. *J Biol Chem* **274**, 26946–26955.

Garner M (2002). Na, K-ATPase in the nuclear envelope regulates Na^+: K^+ gradients in hepatocyte nuclei. *J Membr Biol* **187**, 97–115.

Hibino H, Horio Y, Inanobe A, Doi K, Ito M, Yamada M, Gotow T, Uchiyama Y, Kawamura M, Kubo T & Kurachi Y (1997). An ATP-dependent inwardly rectifying potassium channel, K_{AB}-2 (Kir4.1), in cochlear stria vascularis of inner ear: its specific subcellular localization and correlation with the formation of endocochlear potential. *J Neurosci* **17**, 4711–4721.

Hibino H & Kurachi Y (2006). Molecular and physiological bases of the K^+ circulation in the mammalian inner ear. *Physiology (Bethesda)* **21**, 336–345.

Hibino H, Nin F, Tsuzuki C & Kurachi Y (2010). How is the highly positive endocochlear potential formed? The specific architecture of the stria vascularis and the roles of the ion-transport apparatus. *Pflugers Arch* **459**, 521–533.

Higashiyama K, Takeuchi S, Azuma H, Sawada S, Kakigi A & Takeda T (2010). Ouabain-induced vacuolar formation in marginal cells in the stria vascularis is dependent on perilymphatic Na^+. *ORL J Otorhinolaryngol Relat Spec* **71**(Suppl 1), 57–66.

Higashiyama K, Takeuchi S, Azuma H, Sawada S, Yamakawa K, Kakigi A & Takeda T (2003). Bumetanide-induced enlargement of the intercellular space in the stria vascularis critically depends on Na^+ transport. *Hearing Res* **186**, 1–9.

Hinojosa R & Rodriguez-Echandia EL (1966). The fine structure of the stria vascularis of the cat inner ear. *Am J Anat* **118**, 631–663.

Hudspeth AJ (1989). How the ear's works work. *Nature* **341**, 397–404.

Ikeda K & Morizono T (1989). Electrochemical profiles for monovalent ions in the stria vascularis: cellular model of ion transport mechanisms. *Hearing Res* **39**, 279–286.

Kikuchi T, Adams JC, Miyabe Y, So E & Kobayashi T (2000). Potassium ion recycling pathway via gap junction systems in the mammalian cochlea and its interruption in hereditary nonsyndromic deafness. *Med Electron Microsc* **33**, 51–56.

Kikuchi T, Kimura RS, Paul DL & Adams JC (1995). Gap junctions in the rat cochlea: immunohistochemical and ultrastructural analysis. *Anat Embryol* **191**, 101–118.

Komune S, Huangfu M & Snow JB, Jr (1985). A possible site of production of the negative endocochlear DC potential. *Hearing Res* **18**, 153–158.

Konishi T & Mendelsohn M (1970). Effect of ouabain on cochlear potentials and endolymph composition in guinea pigs. *Acta Otolaryngol* **69**, 192–199.

Kuijpers W & Bonting SL (1970). The cochlear potentials. I. The effect of ouabain on the cochlear potentials of the guinea pig. *Pflugers Arch* **320**, 348–358.

Kujawa SG, Fallon M, Skelletr RA & Bobbin RP (1996). Time-varying alterations in the f2-f1 DPOAE response to continuous primary stimulation II. Influence of local calcium-dependent mechanisms. *Hearing Res* **97**, 153–164.

Kusakari J, Ise I, Comegys TH, Thalmann I & Thalmann R (1978). Effect of ethacrynic acid, furosemide, and ouabain upon the endolymphatic potential and upon high energy phosphates of the stria vascularis. *Laryngoscope* **88**, 12–37.

Maehara H, Okamura HO, Kobayashi K, Uchida S, Sasaki S & Kitamura K (2003). Expression of CLC-KB gene promoter in the mouse cochlea. *Neuroreport* **14**, 1571–1573.

Marcus DC, Marcus NY & Thalmann R (1981). Changes in cation contents of stria vascularis with ouabain and potassium-free perfusion. *Hearing Res* **4**, 149–160.

Marcus DC, Rokugo M & Thalmann R (1985). Effects of barium and ion substitutions in artificial blood on endocochlear potential. *Hearing Res* **17**, 79–86.

Marcus DC, Wu T, Wangemann P & Kofuji P (2002). KCNJ10 (Kir4.1) potassium channel knockout abolishes endocochlear potential. *Am J Physiol Cell Physiol* **282**, C403–407.

Melichar I & Syka J (1987). Electrophysiological measurements of the stria vascularis potentials *in vivo*. *Hearing Res* **25**, 35–43.

Minowa O, Ikeda K, Sugitani Y, Oshima T, Nakai S, Katori Y, Suzuki M, Furukawa M, Kawase T, Zheng Y, Ogura M, Asada Y, Watanabe K, Yamanaka H, Gotoh S, Nishi-Takeshima M, Sugimoto T, Kikuchi T, Takasaka T & Noda T (1999). Altered cochlear fibrocytes in a mouse model of DFN3 nonsyndromic deafness. *Science* **285**, 1408–1411.

Nin F, Hibino H, Doi K, Suzuki T, Hisa Y & Kurachi Y (2008). The endocochlear potential depends on two K^+ diffusion potentials and an electrical barrier in the stria vascularis of the inner ear. *Proc Natl Acad Sci U S A* **105**, 1751–1756.

Nin F, Hibino H, Murakami S, Suzuki T, Hisa Y & Kurachi Y (2012). Computational model of a circulation current that controls electrochemical properties in the mammalian cochlea. *Proc Natl Acad Sci U S A* **109**, 9191–9196.

Offner FF (1987). Positive endocochlear potential: mechanism of production by marginal cells of stria vascularis. *Hearing Res* **29**, 117–124.

Plontke SK, Biegner T, Kammerer B, Delabar U & Salt AN (2008). Dexamethasone concentration gradients along scala tympani after application to the round window membrane. *Otol Neurotol* **29**, 401–406.

Qu C, Liang F, Hu W, Shen Z, Spicer SS & Schulte BA (2006). Expression of CLC-K chloride channels in the rat cochlea. *Hearing Res* **213**, 79–87.

Qu C, Liang F, Smythe NM & Schulte BA (2007). Identification of ClC-2 and CIC-K2 chloride channels in cultured rat type IV spiral ligament fibrocytes. *J Assoc Res Otolaryngol* **8**, 205–219.

Rickheit G, Maier H, Strenzke N, Andreescu CE, De Zeeuw CI, Muenscher A, Zdebik AA & Jentsch TJ (2008). Endocochlear potential depends on Cl^- channels: mechanism underlying deafness in Bartter syndrome IV. *EMBO J* **27**, 2907–2917.

Sage CL & Marcus DC (2001). Immunolocalization of ClC-K chloride channel in strial marginal cells and vestibular dark cells. *Hearing Res* **160**, 1–9.

Sakagami M, Fukazawa K, Matsunaga T, Fujita H, Mori N, Takumi T, Ohkubo H & Nakanishi S (1991). Cellular localization of rat I_{sk} protein in the stria vascularis by immunohistochemical observation. *Hearing Res* **56**, 168–172.

Sakaguchi N, Crouch JJ, Lytle C & Schulte BA (1998). Na-K-Cl cotransporter expression in the developing and senescent gerbil cochlea. *Hearing Res* **118**, 114–122.

Salt AN, Melichar I & Thalmann R (1987). Mechanisms of endocochlear potential generation by stria vascularis. *Laryngoscope* **97**, 984–991.

Schulte BA & Adams JC (1989). Distribution of immunoreactive Na^+,K^+-ATPase in gerbil cochlea. *J Histochem Cytochem* **37**, 127–134.

Schulte BA & Steel KP (1994). Expression of α and β subunit isoforms of Na,K-ATPase in the mouse inner ear and changes with mutations at the W^v or Sl^d loci. *Hearing Res* **78**, 65–76.

Sellick PM & Johnstone BM (1974). Differential effects of ouabain and ethacrynic acid on the labyrinthine potentials. *Pflugers Arch* **352**, 339–350.

Shen Z & Marcus DC (1998). Divalent cations inhibit IsK/KvLQT1 channels in excised membrane patches of strial marginal cells. *Hearing Res* **123**, 157–167.

Shibata T, Hibino H, Doi K, Suzuki T, Hisa Y & Kurachi Y (2006). Gastric type H^+,K^+-ATPase in the cochlear lateral wall is critically involved in formation of the endocochlear potential. *Am J Physiol Cell Physiol* **291**, C1038–C1048.

Shindo M, Miyamoto M, Abe N, Shida S, Murakami Y & Imai Y (1992). Dependence of endocochlear potential on basolateral Na^+ and Cl^- concentration: a study using vascular and perilymph perfusion. *Jpn J Physiol* **42**, 617–630.

Shugyo A, Mori N & Matsunaga T (1990). A comparison of the reduction in the K^+ activity of the scala media produced by furosemide and ouabain. *Eur Arch Otorhinolaryngol* **248**, 79–81.

Slepecky NB (1996). Cochlear structure. In *The cochlea*, ed. Dallos P, Popper AN & Fay RR, pp. 44–129. Springer, New York.

Spicer SS & Schulte BA (1996). The fine structure of spiral ligament cells relates to ion return to the stria and varies with place-frequency. *Hearing Res* **100**, 80–100.

Spicer SS & Schulte BA (2002). Spiral ligament pathology in quiet-aged gerbils. *Hearing Res* **172**, 172–185.

Spicer SS & Schulte BA (2005). Novel structures in marginal and intermediate cells presumably relate to functions of apical versus basal strial strata. *Hearing Res* **200**, 87–101.

Sunose H, Ikeda K, Suzuki M & Takasaka T (1994). Voltage-activated K channel in luminal membrane of marginal cells of stria vascularis dissected from guinea pig. *Hearing Res* **80**, 86–92.

Suzuki M, Kikuchi T & Ikeda K (2004). Endocochlear potential and endolymphatic K^+ changes induced by gap junction blockers. *Acta Otolaryngol* **124**, 902–906.

Takahashi T & Kimura RS (1970). The ultrastructure of the spiral ligament in the Rhesus monkey. *Acta Otolaryngol* **69**, 46–60.

Takeuchi S & Ando M (1998). Inwardly rectifying K^+ currents in intermediate cells in the cochlea of gerbils: a possible contribution to the endocochlear potential. *Neurosci Lett* **247**, 175–178.

Takeuchi S, Ando M & Kakigi A (2000). Mechanism generating endocochlear potential: role played by intermediate cells in stria vascularis. *Biophys J* **79**, 2572–2582.

Takeuchi S, Ando M, Kozakura K, Saito H & Irimajiri A (1995). Ion channels in basolateral membrane of marginal cells dissociated from gerbil stria vascularis. *Hearing Res* **83**, 89–100.

Takeuchi S, Marcus DC & Wangemann P (1992). Ca^{2+}-activated nonselective cation, maxi K^+ and Cl^- channels in apical membrane of marginal cells of stria vascularis. *Hearing Res* **61**, 86–96.

Tasaki I & Spyropoulos CS (1959). Stria vascularis as source of endocochlear potential. *J Neurophysiol* **22**, 149–155.

Ueno A, Tanaka K & Katori M (1982). Possible involvement of thromboxane in bronchoconstrictive and hypertensive effects of LTC4 and LTD4 in guinea pigs. *Prostaglandins* **23**, 865–880.

von Békésy G (1952). DC resting potentials inside the cochlear partition. *J Acoust Soc Am* **24**, 72.

Wangemann P (1995). Comparison of ion transport mechanisms between vestibular dark cells and strial marginal cells. *Hearing Res* **90**, 149–157.

Wangemann P (2002). K^+ cycling and the endocochlear potential. *Hearing Res* **165**, 1–9.

Wangemann P (2006). Supporting sensory transduction: cochlear fluid homeostasis and the endocochlear potential. *J Physiol* **576**, 11–21.

Wangemann P, Liu J & Marcus DC (1995). Ion transport mechanisms responsible for K^+ secretion and the transepithelial voltage across marginal cells of stria vascularis *in vitro*. *Hearing Res* **84**, 19–29.

Xia A, Kikuchi T, Hozawa K, Katori Y & Takasaka T (1999). Expression of connexin 26 and Na,K-ATPase in the developing mouse cochlear lateral wall: functional implications. *Brain Res* **846**, 106–111.

Zdebik AA, Wangemann P & Jentsch TJ (2009). Potassium ion movement in the inner ear: insights from genetic disease and mouse models. *Physiology (Bethesda)* **24**, 307–316.

Additional information

Competing interests

None.

Author contributions

H.H., Y.H., G.O., S.K. and Y.K. designed and directed the study; N.A., T.Y., F.N. and S.Y. performed the experiments; N.A., T.Y. and T.S. analysed the data; and H.H., G.O., S.K. and Y.K. wrote the manuscript. All authors approved the manuscript.

Funding

This work was supported by the following research grants and funds: Grant-in-Aid for Scientific Research B 22390047 and 25293058 (to HH), Grant-in-Aid for Scientific Research on Innovative Areas 22136002 (to YK) and 25136704 (to F.N.), the Global COE Program 'in silico medicine' at Osaka University (to H.H., F.N., Y.K.), and a grant for 'Research and Development of Next-Generation Integrated Life Simulation Software' (to Y.K.), from the Ministry of Education, Culture, Sport, Science and Technology of Japan, the Senri Life Science Foundation (to H.H.), the Ichiro Kanehara Foundation for the Promotion of Medical Sciences and Medical Care (to H.H.), the Mochida Memorial Foundation for Medical and Pharmaceutical Research (to H.H.), the NOVARTIS Foundation (Japan) for the Promotion of Science (to H.H.), the Takeda Science Foundation (to H.H.), the Naito Foundation (to H.H.), Yujin Memorial Grant (to H.H.), the Salt Science Research Foundation (to F.N.), and a Grant for Promotion of Niigata University Research Projects (24A006) (to H.H.).

Acknowledgements

We thank Drs A. J. Hudspeth, Jonathan A. N. Fisher (The Rockefeller University) and Ian Findlay (Université François-Rabelais) for their critical reading of the text.